

radicals. This requirement represents a major drawback in terms of atom economy and waste production.

To address this limitation, Nicewicz and MacMillan have investigated ruthenium bipyridine complexes, which are well-established photoredox catalysts. Under irradiation with blue light, tris(bipyridine)ruthenium(II), Ru(bpy)<sub>3</sub><sup>2+</sup>, forms a more reactive species, \*Ru(bpy)<sub>3</sub><sup>2+</sup>, an excited state in which an electron on the metal transfers to the bpy ligand, where it has enhanced oxidative and reducing power relative to the ground state (9).

Nicewicz and MacMillan elegantly combined this photoredox process (see the figure, blue shading) with organo-SOMO catalysis so that the desired transformation can occur in the correct sequence to generate enolate radicals by a reductive process, and, after coupling with the chiral enamine, oxidize the reaction product. Here, the radical needed in the organo-SOMO catalysis is obtained by a one-electron transfer that reduces an  $\alpha$ -bromo-carbonyl compound with a Ru(I) species, Ru(bpy)<sub>3</sub><sup>+</sup>. The enolate radical possesses an electrophilic character and adds efficiently to the electron-rich chiral enamine (the aldehyde-organocatalyst condensation product) to form an intermediate 1-aminoalkyl radical.

This radical is readily oxidized by the excited \*Ru(bpy)<sub>3</sub><sup>2+</sup> back to the corresponding iminium ion, which upon hydrolysis yields the final product; the oxidation step also regenerates the Ru(bpy)<sub>3</sub><sup>+</sup> ion so that the photoredox catalytic cycle can begin again.

A key feature is that the alkylation step proceeds stereoselectively because of the presence of the chiral secondary amine organocatalyst, which, after condensation with the aldehyde, gives an enamine that helps direct the approach of the incoming radical. Despite the delicately intertwined organo-photoredox catalytic cycles, this reaction is technically simple. It can be performed even with a household 15-W fluorescent light, with no external heating or cooling of the reaction mixture. For example, typical reaction conditions use a relatively high organocatalyst loading (20 mol %) with a minute amount of the photoredox catalyst (0.5 mol %). Indeed, alkylation of a series of aliphatic aldehydes with bromomalonates,  $\alpha$ -bromoesters, and  $\alpha$ -bromo- $\beta$ -ketoesters occurs in excellent yield (63 to 93%) and with high stereochemical control (enantiomeric excess up to 99%) in all cases, even where two stereocenters are created (see the figure, upper right panel).

The selectivities for one enantiomer rival those observed for the classical ionic and concerted reactions, dispelling the previous notion that the high reactivity of radicals precludes their use in catalytic asymmetric synthesis. The cooperation of organo-SOMO catalysis and photoredox catalysis offers many possibilities for asymmetric transformations. A burgeoning field of research is likely to emerge from this seminal work.

#### References

1. D. A. Nicewicz, D. W. C. MacMillan, *Science* **322**, 77 (2008); published online 4 September 2008 (10.1126/science.1161976).
2. S. Bräse, M. Christmann, Eds., *Asymmetric Synthesis—The Essentials* (Wiley-VCH, Weinheim, Germany, 2007).
3. E. N. Jacobsen, A. Pfaltz, H. Yamamoto, Eds., *Comprehensive Asymmetric Catalysis I–III with Supplements 1 and 2* (Springer, Berlin, 2004).
4. For an intramolecular alkylation reaction, see N. Vignola, B. List, *J. Am. Chem. Soc.* **126**, 450 (2004).
5. T. D. Beeson, A. Mastracchio, J.-B. Hong, K. Ashton, D. W. C. MacMillan, *Science* **316**, 582 (2007); published online 28 March 2007 (10.1126/science.1142696).
6. H. Y. Jang, J. B. Hong, D. W. C. MacMillan, *J. Am. Chem. Soc.* **129**, 7004 (2007).
7. H. Kim, D. W. C. MacMillan, *J. Am. Chem. Soc.* **130**, 398 (2008).
8. M. P. Sibi, M. Hasegawa, *J. Am. Chem. Soc.* **129**, 4124 (2007).
9. A. Juris *et al.*, *Coord. Chem. Rev.* **84**, 85 (1988).

10.1126/science.1164403

## BIOCHEMISTRY

# Not Comparable, But Complementary

Lars Juhl Jensen<sup>1,2</sup> and Peer Bork<sup>1,3</sup>

It took many years between the introduction of DNA sequencing technologies in the mid-1970s and completion of the first genome sequences in the mid-1990s. Connecting the one-dimensional “parts lists” encoded within genomes—the proteins—into two-dimensional interaction maps is an even more daunting task, despite the introduction in the late 1980s of the yeast two-hybrid assay to identify protein–protein interactions (1) and high-throughput versions of this technology at the turn of the millennium (2, 3). On page 104 in this issue, Yu *et al.* (4) identify 1809 interactions in the model organism budding yeast, of which more than 1500 are new

relative to the early yeast two-hybrid studies (2, 3). Together with the 2770 interactions recently determined by Tarassov *et al.* by a protein complementation assay (5), almost all of which are new, the number of binary interactions has more than tripled relative to earlier analyses (2, 3). These studies bring us closer to a complete map of biophysical interactions in a single organism, and hence to the ultimate goal of functional understanding of the cellular machinery in space and time (6).

To document the quality of the identified interactions, the two groups performed extensive quality assessments, both on an absolute scale and relative to earlier large-scale studies. According to their estimates, only a few percent of the newly identified interactions are false-positives, which is more than an order of magnitude lower than suggested by previous quality assessments of large-scale yeast two-hybrid experiments (7, 8). However, a direct

New studies increase the number of protein-protein interactions but show little overlap. This is not a bad thing, though.

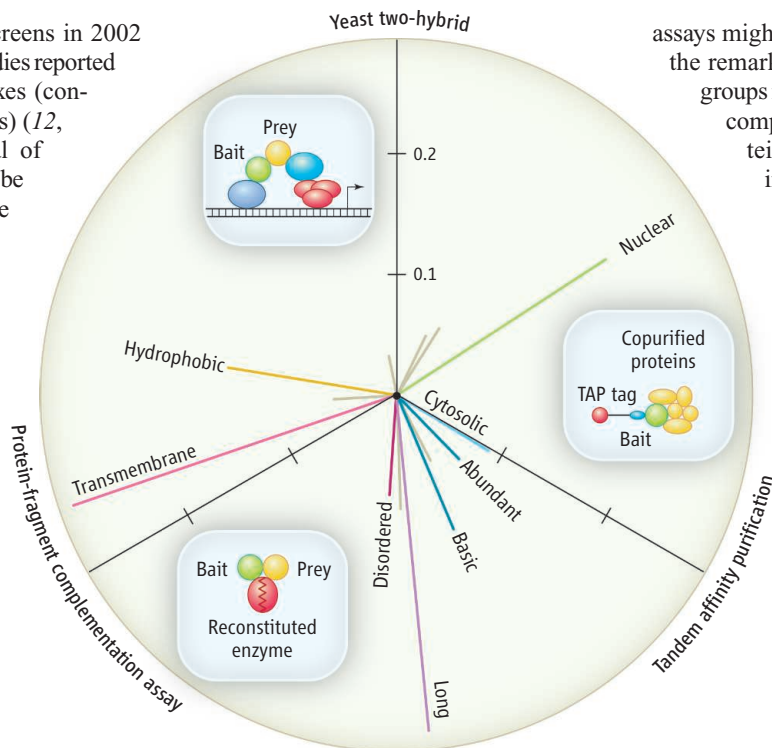
comparison of those numbers is difficult and potentially confusing because each group used a different “gold standard” of known interacting and noninteracting protein pairs. Whereas Yu *et al.* take into account the genome-wide estimate for the number of interacting protein pairs relative to noninteracting ones, the standard used by Tarassov *et al.* is more than 40-fold enriched for interactions. This implicitly lowers the number of false-positives and hence inflates the estimated precision, which drops from 98.2% to around 50% if corrected for this bias. However, the latter value is overly pessimistic because the authors’ reference set disfavors binary interaction assays.

A comparison of numbers becomes even more difficult when considering assays such as tandem affinity purification (9), which copurify proteins that are parts of the same complex. Four years after the first large-scale

<sup>1</sup>European Molecular Biology Laboratory, D-69117 Heidelberg, Germany. <sup>2</sup>The Novo Nordisk Foundation Centre for Protein Research, University of Copenhagen, DK-2200 Copenhagen, Denmark. <sup>3</sup>Max-Delbrück-Centre for Molecular Medicine, D-13092 Berlin, Germany. E-mail: peer.bork@embl.de

protein-protein interaction screens in 2002 (10, 11), two genome-wide studies reported 491 and 547 protein complexes (containing more than two proteins) (12, 13), respectively, and a total of 12,292 protein interactions can be inferred from the respective purifications. Yu *et al.* compared these inferred interactions and the nearly 3000 new and old interactions identified by the yeast two-hybrid assay (2–4) to their binary interaction gold standard and found the two-hybrid assay to be more precise than tandem affinity purification. Conversely, tandem affinity purification performs much better than the two-hybrid assay when using gold standards based on protein complexes (4, 5, 7, 8). These results may seem contradictory, but as alluded to by Yu *et al.*, the approaches are in fact complementary: Binary interaction assays are better at identifying binary interactions, and complex purification assays are better at identifying co-complex interactions (all protein pairs that are part of the same complex) (4). The former provides evidence for direct interactions, whereas the latter allows the binary network to be subdivided into biologically relevant units (that is, complexes).

Although the conceptual difference might account for the poor agreement between the binary and the complex-purification methods, the only 63 interactions common between yeast two-hybrid (2–4) and protein complementation assay (5) screens likely reflect hidden physiochemical constraints inherent to each method. Thus, the different methods might simply capture interactions for different subsets of proteins. This complementation can be confirmed by biases in the types of proteins for which interactions were detected by each assay (see the figure). The most striking trend is that the protein complementation assay has been much better at detecting interactions for transmembrane (and thus hydrophobic) proteins than the other two assays, which Tarassov *et al.* highlight as one of its major strengths. Conversely, the yeast two-hybrid assay and tandem affinity purification both detect interactions for a higher proportion of nuclear proteins, which



**Protein preferences.** The three methods shown for detecting protein interactions function in fundamentally different ways and hence have different physiochemical constraints. Of 15 protein features tested for biases between the sets of proteins for which interactions were identified by each assay, 8 differed significantly (false-positive rate of  $<0.001$ ): presence of transmembrane helices, hydrophobicity, nuclear and cytosolic localization, abundance, predicted isoelectric point, length, and intrinsic disorder. The other seven protein features are shown in gray. The average normalized scores (Z scores) for each of these features are shown, projected onto a plane in which each axis corresponds to one of the three methods for detecting interactions. The length of each line thus represents the strength of the bias.

for the two-hybrid screen is to be expected, because the assay inherently functions inside the nucleus. Notably, interactions from low-throughput studies (14) are similarly biased toward nuclear proteins compared to all yeast proteins. Long proteins, unstructured proteins, and proteins with high isoelectric points are underrepresented among the interactions detected by the yeast two-hybrid assay, whereas tandem affinity purification shows a weak but statistically significant preference for abundant proteins and cytosolic proteins, as shown in the original studies (12, 13), many of which form large stable complexes.

Because the tandem affinity purification approach is close to saturation in terms of protein coverage and, with the study by Yu *et al.*, most yeast proteins have now also been subjected to the two-hybrid assay, the apparent methodological complementation might suggest ways to improve the binary interaction map, because proteins amenable to a certain assay can be examined in greater depth. To improve coverage of interactions, numerous protein-specific optimizations of the existing

assays might be necessary in the future, and the remarkable progress reported by both groups might be the last big step toward a complete catalog of all possible protein–protein interactions in budding yeast, which are estimated to number between 18,000 (4) and 30,000 (7, 8).

Despite the challenging task of characterizing the complete binary “interactome,” it is only a static, two-dimensional representation, because the interactions will never all happen at the same time in the same place. Spatial and temporal data will therefore be needed to decipher where and when an interaction takes place; for example, the interaction network changes considerably during the cell division cycle or other dynamic processes (15). Furthermore, interactions among proteins constitute only one part of the interactome, because associations to other biopolymers (including DNA and RNA), large lipids, and small molecules have to be considered. Finally, the directionality and functionality of the interactions need to be considered as observed, for example, in signaling networks. The growing high-quality interaction map of a model organism, highlighted by Yu *et al.* and Tarassov *et al.* provides the first layer of context to the “parts lists” and lays the foundation for integrating additional spatial, temporal, and functional dimensions necessary for a comprehensive understanding of the eukaryotic cell.

#### References

1. S. Fields, O. Song, *Nature* **340**, 245 (1989).
2. T. Ito *et al.*, *Proc. Natl. Acad. Sci. U.S.A.* **97**, 1143 (2000).
3. P. Uetz *et al.*, *Nature* **403**, 623 (2000).
4. H. Yu *et al.*, *Science* **322**, 104 (2008); published online 21 August 2008 (10.1126/science.1158684).
5. K. Tarassov *et al.*, *Science* **320**, 1465 (2008).
6. P. Bork, L. Serrano, *Cell* **121**, 507 (2005).
7. C. von Mering *et al.*, *Nature* **417**, 399 (2002).
8. J. S. Bader, A. Chaudhuri, J. M. Rothberg, J. Chant, *Nat. Biotechnol.* **22**, 78 (2004).
9. G. Rigaut *et al.*, *Nat. Biotechnol.* **17**, 1030 (1999).
10. A.-C. Gavin *et al.*, *Nature* **415**, 141 (2002).
11. Y. Ho *et al.*, *Nature* **415**, 180 (2002).
12. A.-C. Gavin *et al.*, *Nature* **440**, 631 (2006).
13. N. J. Krogan *et al.*, *Nature* **440**, 637 (2006).
14. T. Reguly *et al.*, *J. Biol.* **5**, 11 (2006).
15. U. de Lichtenberg, L. J. Jensen, S. Brunak, P. Bork, *Science* **307**, 724 (2005).

10.1126/science.1164801